Reliability Evaluation with Wind Turbines and Photovoltaic Panels

Angel Andrés Recalde, Member, IEEE
Facultad de Ingeniería en Electricidad y Computación
Escuela Superior Politécnica del Litoral
Guayaquil, Ecuador
arecalde@espol.edu.ec

Tapan Kumar Saha, Senior Member, IEEE
Mehdi Mosadeghy, Student Member, IEEE
School of Information Technology & Electrical Engineering
The University of Queensland
Brisbane, Australia
saha@itee.uq.edu.au, m.mosadeghy@uq.edu.au

***Abstract*—Deployment of renewable energies in networks can affect their reliability and security. This paper presents a reliability evaluation methodology in the presence of wind turbines and photovoltaic panels illustrated with IEEE-RBTS system chosen for study. The aggregated clean resources feed load points in micro grid configuration. The use of analytical methods provide partial information of reliability indices attributes due to the fact that stochastic characteristics of renewable energy are not thoroughly considered in the traditional radial topology. Thus, a Monte Carlo technique with state duration sampling simulation is applied in order to achieve a detailed analysis of reliability performance of the system. Renewables variability, periodicity, intermittency and typical distribution demand are also considered. This elaborated combination of constraints in the network is possible through the use of a dedicated computer algorithm developed by the authors and presented in this paper.**

***Index Terms*—distributed power generation, micro grid, Monte Carlo simulation, power distribution, power system reliability.**

I. Nomenclature

SAIFI – System Average Interruption Frequency Index
SAIDI – System Average Interruption Duration Index
EENS – Expected Energy Not Supplied
ASAI – Average System Availability Index
IEB, ICB – Interrupted Energy Benefit, Cost Benefit
DG – Distributed Generation

II. Introduction

With the advent of renewable energy DG, it is important to reinvestigate reliability and stability under challenging scenarios [1]. Bidirectional power flow in distribution systems stands inevitably as DGs are connected closer to load points. Hence, utility companies face modernization and restructuring processes towards active network and smart grid concepts adoption supported by execution of advanced distribution and outage management systems to maximize consumer's benefits, energy quality and availability, thus adapting their networks to novel demanding conditions. Consequently, evaluation tools need to handle additional foreseen operation level complexities. Reliability analytical methods are limited in considering these operational constraints completely, i.e. stochastic nature of renewable DG power source, dynamic demand, load shedding schemes, distributed energy location, and others of uttermost importance. However, newer assessment methods and computer simulation algorithms should manipulate realistic assets features and modes of operation in order to model variability, periodicity, intermittency and non-linear characteristics completely. Several upgrading schemes and numerical methods for reliability evaluation have been developed. In [2] a loop path selection alleviates imbalanced load and minimize losses, in [3] minimal tie sets with Petri nets is proposed for circuit minimal tie set identification. The results obtained are suitable for offline comparison of alternative network designs. System reliability indices specify analysis parameters for proper justification of investment options. Some approaches compare the degree of improvement incorporating alternate DG system in island mode [4] or micro grid configuration [5] and others perform economic and worth assessment of energy cost and monetary losses [6]. DG capacity thresholds beyond which there are no significant reliability contributions are found in [7] using IEB and ICB. Nevertheless, accurate studies request updated demand forecasts and national development reports to support the validity of results and correctness of conclusions. Monte Carlo simulation [8]-[11] has been extensively used for complex reliability analysis. It can handle multistate components, stochastic processes, and probabilistic models; hence it is chosen in this paper. Chronological Monte Carlo is selected due to its capacity in building sequential transitions processes through assets synthetic history profiles generation [11]. In this study, IEEE-RBTS network [12] accommodates stand-alone DG, i.e. wind turbines and photovoltaic panels in micro grid configuration. The service connections proposed assume a fully reliable automation and protection systems for switching events. Section III describes DG output power, demand and assets models. The Monte Carlo simulation method is explained in Section IV. In Section V, the effect of integrating renewable DG on the reliability of IEEE-RBTS system is evaluated in two different scenarios. Wind speed

978-1-4799-6251-8/14/$31.00 ©2014 IEEE

historical data of meteorological station ST032040 Townsville Airport and solar radiation from ST039083 Rockhampton Airport in Queensland State, Australia, have been utilized in this study. Finally, results have been discussed in Section VI and conclusions are summarized in Section VII.

III. Components Models

IEEE–RBTS network has been extensively investigated in reliability studies [12]. Nevertheless, medium sized renewable DG systems have been directly added at 11kV voltage level in simple micro grid configuration, as shown in Fig. 1. DGs sizes range from 200kW up to 3000kW, as available commercially. Its operation can be outlined as below:

- At normal mode, main supply matches the system demand; DG energy is consumed locally, any DG surplus power turns to main grid.
- On a failure event, the faulty line section or distributor is isolated and enabled load demand (total or partial) is assisted by available DGs energy. All failures are considered as short-circuits, lateral fuses blow on a trip event, and disconnect isolators provide reclosing actions under load transfers [13].
- After clearing the fault, the system is reestablished to the normal mode state. DGs switch to join main grid again.

Artificial history profiles are generated for all the system components in the base case and assisted configurations shown in Fig. 2. In the case of renewable DGs, time series models are developed to define the ST032040 and ST039083 Australian sites specific wind speed and solar radiation patterns and calculate power profiles. A dynamic load model considering diversity, forecast and typical profiles resemble realistic demand projections.

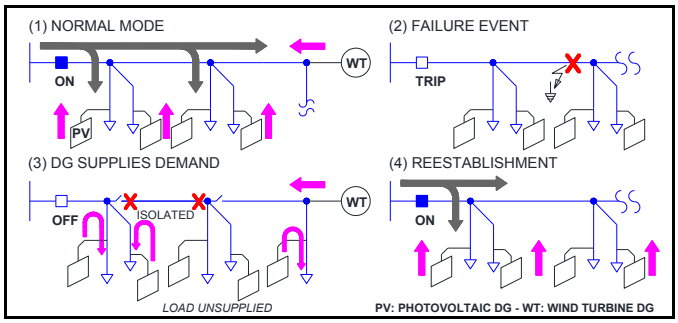

Fig. 1. DG supply. After a failure event (2), the network isolates the fault and reconfigures itself; load is supplied by renewables DG (3).

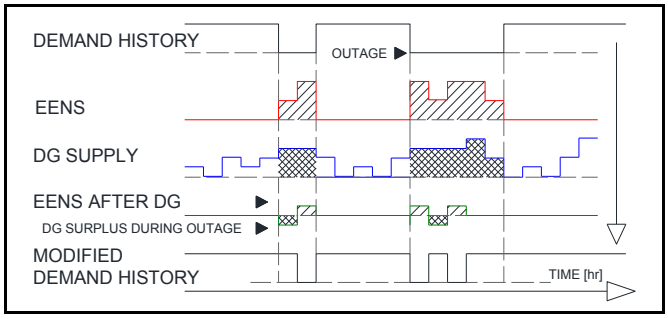

Fig. 2. DG contribution. The original demand history (top) is modified (bottom) after load points were supplied by renewable DG.

A. Wind speed model and wind turbine output

Wind turbine WT output power depends on wind speed and wind turbine parameters expressed as in the following non-linear relationship [14].

$$P_{WT} = \begin{cases} (A + B \cdot v_t + C \cdot v_t^2) P_r \\ P_r \end{cases} \quad (1)$$

Where the second order polynomial corresponds to wind speeds $v_{ci} \le v_t \le v_r$ and the output is constant in $v_r \le v_t \le v_{co}$; v_{ci}, v_r, and v_{co} are the cut-in, rated, and cut-out wind speeds respectively, and P_r is the kW capacity of the wind turbine chosen; outside the aforementioned intervals, the output is 0 due to mechanical and operational constraints. The A, B, and C coefficients depend only on v_{ci}, v_r, and v_{co} [14]. Historical wind speed hourly data is needed to build the time series model directly [15], and then simulate numerous chronologically ordered synthetic wind speed profiles that replace v_t in (1). The procedure is outlined below.

1. A stationary residual vector y representing a stochastic process of the hourly wind speed is calculated with average μ and standard deviation σ vectors from original wind speed hourly data y_{DATA}.

$$y = (y_{DATA} - \mu)/\sigma \quad (2)$$

2. Vector y can be modeled with an auto-regressive moving average *ARMA* process [15], depicted in a polynomial y_t.

$$y_t = \varphi_1 y_{t-1} + \cdots + \varphi_p y_{t-p} + \alpha_t - \theta_1 \alpha_{t-1} + \cdots + \theta_q \alpha_{t-q} \quad (3)$$

Where φ_i (i = 1, 2,…, p) and θ_i (j = 1, 2,…, q) are the auto-regressive and moving average parameters respectively; α_t is a normal white noise process with normal independent distribution (0, σ^2_a). The optimum p, q is found through the Bayesian Information Criterion (*BIC*), which resolves the over-fitting problem as well [16].

3. Synthetic wind speed profiles v_t are simulated using (4). The root mean square *NRMSD* and mean bias difference *NMBD* can validate the results [17]. Replacing (4) into (1) and specifying wind turbine parameters, power output profiles can be generated as shown in Fig. 3. Self-coordination control for the wind turbine operation is considered.

$$v_t = \mu + \sigma y_t \quad (4)$$

B. Solar radiation model and photovoltaic panel output

Solar radiation is affected by daily and seasonal cyclical variations. Such periodicities can be modeled separately and combined in the last step. Fourier transformation defines all the cyclical patterns [17] while time series handles the stochastic characteristic with an *ARMA* (p, 0) process. The procedure is similar to the previous one explained above [18].

1. Fourier transformations μ_F and σ_F of daily solar radiation average μ and standard deviation σ vectors containing only the fundamental frequency component represents seasonal periodicity. Another Fourier transformation pair for hourly variability includes up to the 6th harmonic, approximating nighttime radiance to 0.
2. With the stationary residual vector using μ_F and σ_F in (2), perform an auto-regressive process of degree 1, i.e.

$y_t = \varphi_1 y_{t-1} + \alpha_t$. Verify that normal and partial autocorrelation have continuous decaying trend.

3. The synthetic solar seasonal and daily radiation profiles g_t can be calculated separately using μ_F and σ_F in (4). A final step merges both periodicity models into one appropriate hourly solar radiation model. Again, it can be validated with *NRMSD* and *NMBD* [17]. An example of an artificial photovoltaic panel output profile is shown in Fig. 3

Photovoltaic PV panel output power depends on the solar radiation level and also relies on the manufacturer's efficiency [19]. This non-linear relation can be written as in (5).

$$P_{PV} = \begin{cases} \frac{\eta_C}{K_C} g_t^2 P_r & 0 \le g_t < K_C \\ \eta_C g_t P_r & K_C \le g_t < STC \\ \eta_C P_r & g_t \ge STC \end{cases} \quad (5)$$

Where g_t is solar radiation, η_C rated efficiency, K_C boundary radiation point (500-800 W/m^2), P_r nominal capacity of photovoltaic unit in kW, and *STC* is the standard radiation point (1000 W/m^2) [19]. Photovoltaic panels range from 4kW to 70kW in urban areas, but in the IEEE-RBTS the customers capacities cumulate in a single load represented in a lateral distributor load point.

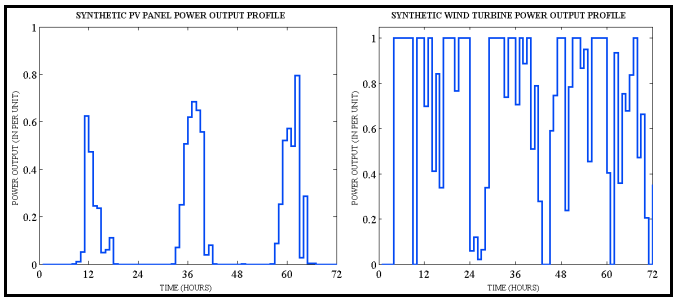

Fig. 3. Synthetic wind turbine and PV panel power output power profile.

C. Distribution load and demand model

Loads in urban distribution networks can be classified in residential, institutional, and commercial types [12]. Their demand curves reflect particular energy usage, climate factors, population growth, and economic development. IEEE-RBTS maximum demands are individually combined with IEEE Reliability Test System-1996 seasonal and daily profiles [20], annual forecast national demand growth figures, and typical 24 hour load curves per load type [21]. Thus, the Monte Carlo simulation conserves realistic demand behavior and accuracy on the results is improved. With the aim of Australian National Reports on energy demand, dwelling projection, state budget, and public sector [22], the 2013 annual growth forecast figures for the simulation used in this study are: energy demand 2.9%, number of customers (dwellings) 2.13%, commercial 4%, and public institutional 3.04%.

D. Electrical assets and components models

Distribution assets are commonly two-state modeled with exponentially distributed failure rates but some components are multistate. For instance, overhead lines have two-state models while transformers include repair, replacement and isolation states. DGs comprehend multistate models with exponentially distributed failure rates and exponentially or log-normal distributed repair times [10]. Circuit breakers, fuses and disconnection switches are considered fully reliable devices. Table I shows failure rates and repair times for main components in the IEEE-RBTS network.

TABLE I
COMPONENTS FAILURE RATES AND SWITCHING TIMES

Description	*Failure rate λ (f/yr.)*	*Switching times*
Overhead lines	0.06500	5h repair, 1h isolate
Dist. transformer	0.01500	200h repair
Wind turbine	0.00136	420h repair
Photovoltaic panel	0.00038	34h repair

E. Interrupted energy cost model

The monetary cost per failure event depends mainly on the type of load, location, fault duration, and market situation. Whenever updated government statistics are not available, well-documented academic studies [13] are used as a reference. This model consists of a matrix of monetary losses versus interruption duration for each distribution load type.

IV. MONTE CARLO SIMULATION

The chronological Monte Carlo simulation generates hourly synthetic history profiles over *n* years and *p* periods for every system component with state duration sampling approach. Then instantaneous reliability index averages and probability distributions can be calculated and analyzed. In fact, index averages (6) are vital in the decision-making process for supporting new investment plans.

$$x_{MC} = \left(\sum_{i=1}^{n} x_i\right)/n \quad (6)$$

Where n is the number of years (trials), x_i is the index annual value in year i, and x_{MC} is the annual average. The initial conditions of the problem are: a) increasing dynamic demand, b) constant DG capacity, c) no energy storage possibility. The inputs of the algorithm are the planning constraints shown in Table II, the assets and DG models, demand and interrupted energy cost models, and the topology of the IEEE–RBTS network.

TABLE II
MONTE CARLO SIMULATION PARAMETERS

Project lifetime	20 yr.
Years of evaluation/year-samples (trials)	1600 yr.-s.
Wind turbine arrangement	1or *n*
Failure probabilistic distribution	Exponential

The simulation core sequence of the algorithm written by the authors is outlined below.

1. IEEE-RBTS network topology, forecast demand figures, and DGs parameter initialization.
2. Assets artificial histories and renewable DGs synthetic power output profiles generation.
3. Load point demands artificial histories generation. Loads have different levels on each hourly time interval.
4. With all synthetic history vectors in chronological order, energy indices are calculated, i.e. EENS. Original base case is compared to the assisting DGs scenario. After a fault and during restoration, the available DGs energy

limits the load transfer capability at each time interval and a load shedding scheme prioritizes load points with higher demands. Hence, DGs capacity adequacy supports micro grid formation but its distribution is restrained by network topology limitations.

5. Calculation of system and load reliability indices. The analysis can determine a qualitative reliability adjustment when using medium-scale renewable DGs.

V. Case Studies

Two cases have been evaluated. First case locates one WT per feeder, while in the second case there are as many WTs as lateral distributors. Additionally, in both cases PV panel works in parallel with each load point, thus enhancing the assistance capability. In this paper, positive improvement in reliability stands for a decrement in index magnitudes. For instance, 15% EENS improvement implies that EENS was reduced by 15% with respect to the base case, i.e. no DGs. Renewable DG capacity is sized according to its targeted demand, which can be single load point in the case of PV panels, and total feeder or total lateral distributor demand in the case of WTs. Demands for IEEE-RBTS are: bus B2 20MW, and bus B4 40MW, so the total system demand is 60MW.

A. *Case I - One wind turbine at the end of each feeder*

The results with single WT per feeder are shown in Table III. For bus 2 with wind power solely, EENS gets 6% of improvement but it reaches 27% deploying solar power only. When the DG capacity equals B2 demand with wind and solar power evenly divided, EENS improves up to 20% and higher DG capacities achieves 31% at most. Expected Cost of Energy Interruption (ECOST) experiences reductions as well, i.e. it decreases by more than 22% with high renewable DG penetration. On the other hand, SAIFI and ASAI for B4 follow similar tendencies. The interruption frequency can be cut up to 22% with combined DG capacities up to 20MW total. However, higher DG capacities can reduce SAIFI by 40%. The availability of B4 can be increased by 19% or 21% with large mixed DG penetration.

B. *Case II –Wind turbines at every lateral distributor*

The availability of B2 can be increased up to 24% when there is a high solar power penetration, as shown in Table IV. It can be said that ASAI improves by 12% with different combinations of renewable DGs. On the other side, SAIFI can get as much as 37% of improvement. Nevertheless, wind power solely contributes with a 20% cut on the interruption frequency. Therefore, SAIFI is further enhanced for the same DG capacities. Bus 4 results are shown in Fig. 4. EENS has an overall positive improvement no matter what DG combination is chosen and it reaches around 40% easily. Consequently, EENS is always favored when DG is added to the system. Besides these results, SAIDI exhibits scattered improvements for different DG variants. However, it reaches approximately 13% in most of the cases and 25% maximum. Interestingly, wind power solely can improve the duration of interruptions by 15% with 30MW of DG capacity.

In Fig. 5, annual failure rates of all load points of B2 and B4 are drawn. Generally, failure rates lessen with respect to the base case, except for few load points. Case I and II achieve important improvements in most of the loads, but in some cases the outcomes are not representative.

TABLE III
Reliability Indices Improvements (%) case I, single WT.

BUS 2 (B2, 20 MW)											
EENS		*Wind power (MW)*				**ECOST**		*Wind power (MW)*			
		0	*5*	*10*	*15*			*0*	*5*	*10*	*15*
PV (MW)	*0*	0	2	4	6	*PV (MW)*	*0*	0	2	0	8
	5	7	10	18	27		*5*	0	0	8	21
	10	14	11	20	28		*10*	8	2	10	22
	15	27	14	22	31		*15*	20	3	0	18
BUS 4 (B4, 40 MW)											
SAIFI		*Wind power (MW)*				**ASAI**		*Wind power (MW)*			
		0	*10*	*20*	*30*			*0*	*10*	*20*	*30*
PV (MW)	*0*	0	4	17	30	*PV (MW)*	*0*	0	4	12	16
	10	0	10	7	7		*10*	2	9	4	9
	20	0	16	22	21		*20*	0	12	13	15
	30	2	38	35	40		*30*	2	18	21	19

TABLE IV
Reliability Indices Improvements (%) case II B2, multiple WTs.

SAIFI		*Wind power (MW)*				**ASAI**		*Wind power (MW)*			
		0	*5*	*10*	*15*			*0*	*5*	*10*	*15*
PV (MW)	*0*	0	5	17	20	*PV (MW)*	*0*	0	4	13	15
	5	0	7	9	10		*5*	0	6	8	9
	10	0	19	23	14		*10*	3	10	12	10
	15	0	37	26	30		*15*	0	24	12	19

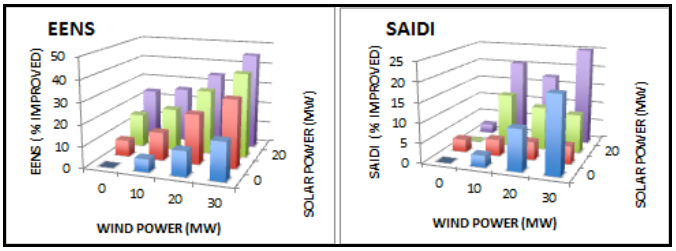

Fig. 4. EENS and SAIDI case II bus 4.

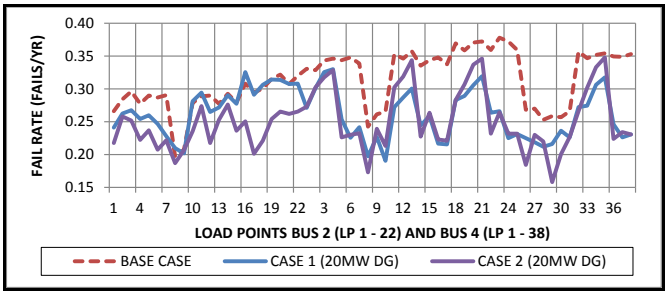

Fig. 5. Failure rates (fails/year) of all B2 and B4 load points

Figure 6 presents IEB and ICB variations for wind power sweep at different levels of solar power penetration for bus 2 Case I and bus 4 Case II. The tendencies shown resemble a second order polynomial, thus their magnitudes can be maximized combining certain DG capacities. For instance, for bus 2 case I with wind power capacity of 10MW under 10MW of solar penetration, IEB reaches 70 kWh/MW while its ICB saves 2750 k$/MW annually, i.e. there is a 70kWh less energy interrupted and 2.75M$ energy benefit annually per MW of installed DG. Although these figures are optimistic, renewable DG deployment faces operational and maintenance costs,

planning restrictions, upgrades for security enhancements, economies of scale, and other constraints that limit the initial impression to start a rapid adoption.

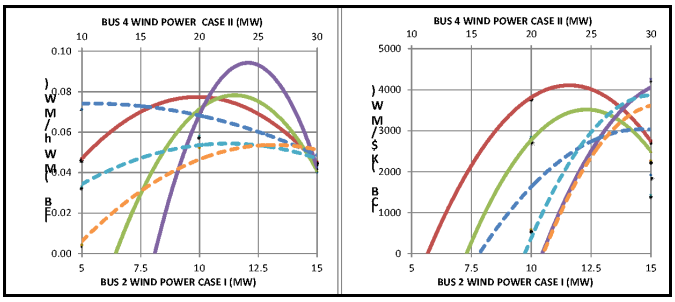

Fig. 6. IEB & ICB for B2 case I and B4 case II – Photovoltaic power for B2 case I: red 5MW, green 10MW, purple 15MW; Photovoltaic power for B4 case II: blue 10MW, cyan 20MW, and orange 30MW.

VI. Discussion

There are positive improvements in reliability and availability when renewable DGs are installed. Their diverse capacities have proven to reduce energy not supplied and failure rate upon a growing dynamic demand. However, the improvement magnitude varies differently for each reliability index. Therefore, it is not possible to minimize energy not supplied, cost benefits, interruption frequency and duration, failure rates and other figures equally for a given combination of wind and solar DG capacities. Nevertheless, such utility company objectives require a compromise in the planning stage of the project. Multi-turbine configurations provide better results and higher reliability than single-turbine cases. Solar power offers higher energy contributions, i.e. EENS and ECOST improve remarkably but SAIFI and SAIDI obtain lower contributions. On the other hand, wind power provides higher contributions to interruption frequency and duration, but lesser to energy not supplied and cost of interruption. Generally, the availability of the system is increased and failure rates and interruption duration shortened with any combination of renewable DGs.

VII. Conclusion

Chronological Monte Carlo simulation with state duration sampling and multistate stochastic approach has been used to evaluate the reliability of the IEEE-RBTS network with wind turbines and photovoltaic panels. Improvement in reliability and availability has been achieved; however, its magnitude depends on the location, renewable DG penetration and configuration, and type of index scrutinized. Higher energy benefits can be accomplished with large penetration of solar power. Any combination of wind and solar renewable distributed generation reduces energy not supplied largely, but interruption frequency and duration figures have different positive impacts depending on the system conditions and renewable DGs deployment level.

References

[1] M. H. Bollen and F. Hassan, *Integration of distributed generation in the power system*, IEEE and John Wiley & Sons, pp.1-3., 2011.

[2] J.C. Kim, S.M. Cho, H.S. Shin, "Advanced power distribution system configuration for Smart Grid" IEEE Trans. on Smart Grid, pp. 353-358, March 2013.

[3] M. Al-Muhaini, G. T. Heydt, "A novel method for evaluating future power distribution system reliability," IEEE Trans. on Power Systems, Vol. 28, No. 3, pp. 3018-3027, August 2013.

[4] G. Wang, Z. Liu, N. Liu, and J. Zhang, "Reliability evaluation of distribution system with distributed generation based on islanding algorithm," *Electric Utility Deregulation and Restructuring and Power Technologies 3rd Conference.,* pp. 2697-2701, April 2008.

[5] M. E. Khodayar, M. Barati, and M. Shahidehpour, "Integration of high reliability distribution system in microgrid operation," IEEE Transactions on Smart Grid, Vol. 3, No. 4, pp. 1997-2006, Dec. 2012.

[6] N. R. Godha, S. R. Deshmukh, and R. V. Dagade, "Application of Monte Carlo simulation for reliability cost/worth analysis of distribution system," *International Conference on Power and Energy Systems*, Dec. 2011.

[7] P. Wang and R. Billinton, "Reliability benefit analysis of adding WTG to a distribution system," IEEE Trans. on Energy Conversion, Vol. 16, No. 2, pp. 134-139, June 2001.

[8] A. A. Alkuhayli, S. Raghavan, B. H. Chowdhury, "Reliability evaluation of distribution systems containing renewable distributed generations," North America Power Symposium, pp. 1-6, Sept. 2012.

[9] Leite da Silva A., Nascimento L., Da Rosa M.A., Issicaba D., Pecas Lopes J.A., "Distributed energy resources impact on distribution system reliability under load transfer restrictions", IEEE Transactions on Smart Grid, Vol. 3, No. 4, pp. 2048-2055, May 2012.

[10] R. Billinton and W. Li, *Reliability assessment of electric power systems using Monte Carlo methods*, Plenum Press, NY & LON, 1994.

[11] R. Billinton and P. Wang, "Teaching distribution system reliability evaluation using Monte Carlo simulation," IEEE Trans. on Power Systems, Vol. 14, No.2, pp. 397-403, May 1999.

[12] R. N. Allan, R. Billinton, I. Sjarief, L. Goel, and K. S. So, "A reliability test system for educational purposes," IEEE Trans. on Power Systems, Vol. 6, No. 2, pp. 813-820, May 1991.

[13] R. Billinton and R. N. Allan, *Reliability evaluation of power systems* (2nd ed.), Plenum Press, New York and London, 1996.

[14] R. Karki, P. Hu, and R. Billinton, "A simplified wind power generation model for reliability evaluation," IEEE Trans. Energy Conversion, Vol. 21, No. 2, pp. 553-540, June 2006.

[15] R. Billinton, H. Chen, and R. Ghajar, "Time series models for reliability evaluation of power systems including wind energy," Elsevier Science, Vol. 36, No. 9, pp. 1253-1261, 1996.

[16] The Mathworks Inc., Choose ARMA lags using BIC, [Online]. Available: mathworks.com.au/help/econ/choose-arma-lags.html.

[17] J. Boland, *Modeling solar radiation at the earth surface: Time series modeling of solar radiation*, Ch. 11, University of South Australia, Mawson Lakes, Springer Berlin Heidelberg, 2008, pp. 283-312.

[18] J. Boland, "Time series analysis of climatic variables," Elsevier Science, Solar Energy, Vol. 55, No. 5, 1995, pp. 377-388.

[19] R. Karki, A. Alferidi, and R. Billinton, "Reliability modeling for evaluating the contribution of photovoltaic in electric power systems," in *37th IEEE Photovoltaic Specialist Conf.,* pp. 1811-1816, June 2011.

[20] C. Grigg, P. Wong, P. Albretch, R. Allan, "The Reliability Test System-1996. A report prepared by the Reliability Test System Task Force", IEEE Trans. on Power Systems, Vol. 14, No. 3, August 1999.

[21] Central Station Engineers of Westinghouse Electric Corp., *Electrical Transmission and Distribution Reference Book,* Westinghouse Electric Corporation, 4th Ed., Ch. 14, pp. 788, 1964.

[22] National Electricity Forecasting Report 2012; Household and Dwelling Projections 2011 Ed. QLD; Queensland State Budget 2012-2013; Queensland Public Service Workforce Characteristic Report 2011-2012, QLD Government at a glance.